3D locomotion based on Divergent Component of Motion

Johannes Englsberger, Christian Ott and Alin Albu-Schäffer

Institute of Robotics and Mechatronics, German Aerospace Center (DLR), Wessling, Germany

johannes.englsberger@dlr.de

1 Introduction

For humanoid robots to be used in real world scenarios, there is a need of robust and simple walking controllers. Many successful LIP based walking control methods have been presented recently [1, 2, 3]. The use of the LIP model for bipedal walking control is restricted to horizontal CoM motions ($z = const.$). We overcome this limitation by extending the concept of Divergent Component of Motion (DCM [4], also called 'Capture Point' [5, 6]) to 3D. Therefore, we introduce the "Enhanced Centroidal Moment Pivot point" (eCMP) and the "Virtual Repellent Point" (VRP), which allow for a intuitive understanding of the robot's CoM dynamics. Based on eCMP, VRP and DCM, we present a method for real-time planning and control of DCM trajectories in 3D (see also [7]). The proposed control architecture was tested in numerous simulations and proves to be very robust.

2 Three-dimensional DCM, eCMP and VRP

Motivated by the performance of 2D Capture Point (= DCM) control [6, 8], we introduce the three-dimensional Divergent Component of Motion (DCM):

$$\boldsymbol{\xi} = \boldsymbol{x} + b\,\dot{\boldsymbol{x}}, \tag{1}$$

where $\boldsymbol{\xi} = [\xi_x, \xi_y, \xi_z]^T$ is the DCM, $\boldsymbol{x} = [x, y, z]^T$ and $\dot{\boldsymbol{x}} = [\dot{x}, \dot{y}, \dot{z}]^T$ are the CoM position and velocity and $b > 0$ is the time-constant of the DCM dynamics. By reordering (1), we directly find the CoM dynamics as

$$\dot{\boldsymbol{x}} = -\frac{1}{b}\,(\boldsymbol{x} - \boldsymbol{\xi}). \tag{2}$$

This shows that the CoM has a stable first order dynamics for $b > 0$ ($\rightarrow$ it follows the DCM). Additionally, we introduce the so called *Enhanced Centroidal Moment Pivot point* (eCMP), which *encodes the external* (e.g. leg-) *forces in a linear force law*, based on the difference of the CoM and the eCMP:

$$\boldsymbol{F}_{ext} = \frac{m}{b^2}\,(\boldsymbol{x} - \boldsymbol{r}_{ecmp}). \tag{3}$$

The eCMP is closely related to the CMP [9], but not restricted to the ground surface. This allows encoding not only the direction of the sum of external forces, but also its magnitude. By introducing the so called Virtual Repellent Point (VRP) as

$$\boldsymbol{r}_{vrp} = \boldsymbol{r}_{ecmp} + \begin{bmatrix} 0 & 0 & b^2 g \end{bmatrix}^T = \boldsymbol{r}_{ecmp} + \begin{bmatrix} 0 & 0 & \Delta z_{vrp} \end{bmatrix}^T, \tag{4}$$

the DCM dynamics can be expressed as

$$\dot{\boldsymbol{\xi}} = \frac{1}{b}\,(\boldsymbol{\xi} - \boldsymbol{r}_{vrp}). \tag{5}$$
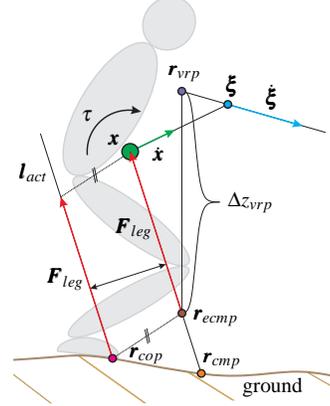

Figure 1: Point correlations for general robot dynamics.

For $b > 0$ the DCM has an unstable first order dynamics (*DCM is "pushed" by the VRP on a straight line*). Figure 1 clarifies the correlations between eCMP, CMP and CoP.

3 Generation of DCM reference

The basic idea is to find a DCM trajectory which corresponds to constant eCMPs in the centers of the preplanned future foot positions $\boldsymbol{r}_{f,i}$ and thus increases the likelihood of feasible leg forces ($\rightarrow$ CoP). Given a desired eCMP-to-VRP height difference Δz_{vrp}, we find according desired VRPs with (4) as

$$\boldsymbol{r}_{vrp,d,i} = \boldsymbol{r}_{f,i} + \begin{bmatrix} 0 & 0 & \Delta z_{vrp} \end{bmatrix}^T \tag{6}$$

With (4), we find the DCM time-constant as $b = \sqrt{\Delta z_{vrp}/g}$. Desired end-of-step DCM locations are found via recursion:

$$\boldsymbol{\xi}_{d,eos,i-1} = \boldsymbol{\xi}_{d,ini,i} = \boldsymbol{r}_{vrp,d,i} + e^{-\frac{t_{step}}{b}}\,(\boldsymbol{\xi}_{d,eos,i} - \boldsymbol{r}_{vrp,d,i}). \tag{7}$$

For $t < t_{step}$, the desired DCM trajectory in time is

$$\boldsymbol{\xi}_d(t) = \boldsymbol{r}_{vrp,d,1} + e^{\frac{t - t_{step}}{b}}(\boldsymbol{\xi}_{d,eos,1} - \boldsymbol{r}_{vrp,d,1}). \tag{8}$$

4 Three-dimensional DCM tracking control

The DCM control law used in the presented work is

$$\boldsymbol{r}_{vrp,c} = \boldsymbol{\xi} + k\,b\,(\boldsymbol{\xi} - \boldsymbol{\xi}_d) - b\,\dot{\boldsymbol{\xi}}_d. \tag{9}$$

It leads to a stable closed loop dynamics for $b > 0$ and $k > 0$. The according desired leg-force can be found as

$$\boldsymbol{F}_{leg,c} = \frac{mg}{\Delta z_{vrp}}\,(\boldsymbol{x} - \underbrace{(\boldsymbol{r}_{vrp,c} - \begin{bmatrix} 0 & 0 & \Delta z_{vrp} \end{bmatrix}^T)}_{\boldsymbol{r}_{ecmp,c}}) \tag{10}$$
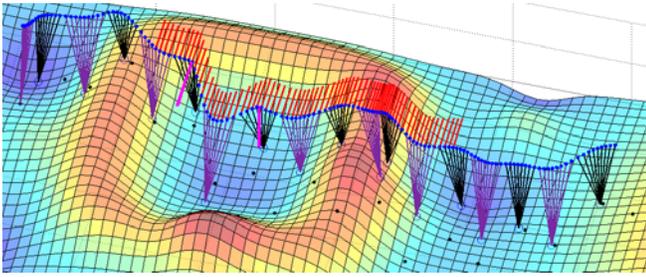
Figure 2: Simulation for Prismatic Inverted Pendulum model [12] (Point mass with two point feet). Robot walks from left to right over rough ($\approx -10cm..+50cm$) terrain. Red and pink lines: continuous (10% of body weight) and impulsive perturbation forces ($\rightarrow \Delta \dot{x} = 1m/s$).

Figure 3: Qualitative comparison of force profiles: a) measurement [13], b) bipedal SLIP [13], c) Linear/Prismatic Inverted Pendulum (LIP/PIP) with instantantaneous single support transitions, d) LIP/PIP with continuous double support transitions

Note that the only equations that are finally needed are (7) and (8) for three-dimensional DCM trajectory generation and (9) and (10) for force-based DCM tracking control. They can easily be computed in real-time on any computer.

5 Features and verification

In addition to the shown equations, we found methods to guarantee feasibility of the finally commanded forces (based on projections of the desired eCMP to feasible regions and use of centroidal momentum [9]). The controller shows high robustness towards external unknown perturbations (constant and impulsive forces) and model inaccuracies. An explicit robustness analysis w.r.t. CoM error, mass estimation error, external forces and actuator force lag showed promising results. In addition to the simulation shown in Fig. 2, the proposed control method has been validated in numerous simulations, amongst others in an OpenHRP [10] simulation of DLR's humanoid TORO passing over a set of stairs of variable height (up to $+12cm$ and $-18cm$). Recently [11], in cooperation with IHMC's robotics lab, we extended the presented methods to guarantee continuous leg forces during double support (similar to [12]) and heel-to-toe shift ($\rightarrow$ toe-off motion).

6 Proposal for discussion

In both biologically inspired [13] and inverted pendulum (linear [14]/prismatic [12]) based works, it has been argued that the correlating leg force profiles and CoM motions fit nicely to the ones observed in nature ($\rightarrow$ force plate/motion capture). Yet, the force profiles for these different template models differ drastically (see Fig. 3). Thus, it may be discussed which one of the two models actually fits natural observations better and which commonalities these models have.

References

[1]   B. Stephens and C. Atkeson, "Push recovery by stepping for humanoid robots with force controlled joints," in *Humanoids*, 2010.

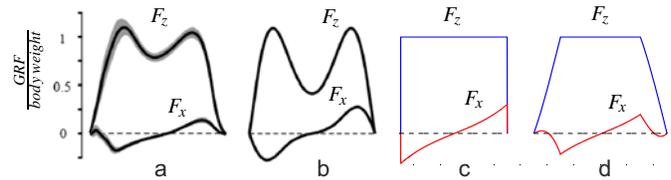[2]   P.-B. Wieber, "Trajectory free linear model predictive control for stable walking in the presence of strong perturbations," in *Humanoids*, 2006.

[3]   S. Kajita, M. Morisawa, K. Miura, S. Nakaoka, K. Harada, K. Kaneko, F. Kanehiro, and K. Yokoi, "Biped walking stabilization based on linear inverted pendulum tracking," in *IROS*, 2010.

[4]   T. Takenaka, T. Matsumoto, and T. Yoshiike, "Real time motion generation and control for biped robot, 1st report: Walking gait pattern generation," in *IROS*, 2009.

[5]   J. Pratt, J. Carff, S. Drakunov, and A. Goswami, "Capture point: A step toward humanoid push recovery," in *Humanoids*, 2006.

[6]   T. Koolen, T. D. Boer, J. Rebula, A. Goswami, and J. E. Pratt, "Capturability-based analysis and control of legged locomotion. part 1: Theory and application to three simple gait models," *IJRR*, 2012.

[7]   J. Englsberger, C. Ott, and A. Albu-Schffer, "Three-dimensional bipedal walking control using divergent component of motion," in *IROS*, 2013.

[8]   J. Englsberger, C. Ott, M. A. Roa, A. Albu-Schäffer, and G. Hirzinger, "Bipedal walking control based on capture point dynamics," in *IROS*, 2011.

[9]   M. B. Popovic, A. Goswami, and H. Herr, "Ground reference points in legged locomotion: Definitions, biological trajectories and control implications," *IJRR*, vol. 24, 2005.

[10]   F. Kanehiro, K. Fujiwara, S. Kajita, K. Yokoi, K. Kaneko, H. Hirukawa, Y. Nakamura, and K. Yamane, "Open architecture humanoid robotics platform," in *ICRA*, 2002.

[11]   J. Englsberger, T. Koolen, S. Bertrand, J. Pratt, C. Ott, and A. Albu-Schäffer, "Trajectory generation for continuous leg forces during double support and heel-to-toe shift based on divergent component of motion," in *IROS 2014 (submit.)*.

[12]   Y. Zhao and L. Sentis, "A three dimensional foot placement planner for locomotion in very rough terrains," in *Humanoids*, 2012.

[13]   H. Geyer, A. Seyfarth, and R. Blickhan, "Compliant leg behaviour explains basic dynamics of walking and running," *Proc. of the Royal Society B: Biological Sciences*, 2006.

[14]   A. L. Hof, "The 'extrapolated center of mass' concept suggests a simple control of balance in walking," *Human Movement Science*, vol. 27, pp. 112–125, 2008.